Smart Pumpless Loop for Micro-Channel Electronic Cooling Using Flat and Enhanced Surfaces

Swaraj Mukherjee and Issam Mudawar

***Abstract*—Two-phase cooling of a square simulated electronic device surface of 21.3 mm side was successfully carried out without the need for a pump. This smart, passive cooling system incorporates a self-enhancing and self-sustaining mechanism, wherein the system inherently enhances its cooling capacity by increasing the velocity of the two-phase mixture along the boiling surface when an increase in heat flux is sensed. Other practical attributes of this pumpless loop are small liquid inventory requirements and absence of the incipient boiling temperature drop. It is shown small surface tension and contact angle render dielectric coolants such as FC-72 ideally suited for flow in narrow gaps. These unique properties are responsible for very small bubble size, precluding any appreciable blockage of the replenishment liquid flow even in narrow gaps. Critical heat flux (CHF) was found to generally increase with decreasing boiler gap. CHF for flat, micro-channel (with 0.2 mm rectangular fins) and mini-channel (with 1.98 mm rectangular fins) surfaces was 4.5, 5.9, and 5.7 times greater than for pool boiling from a flat surface for corresponding gaps. A pressure drop model was formulated to predict coolant mass flow rate, boiling surface inlet and exit velocities, and pressure drop components throughout the loop. The model predictions illustrate the pumpless loop's self-sustaining and self-enhancing attributes, and relate CHF trends to those of the two-phase mixture acceleration along the boiling surface.**

***Index Terms*—Boiling, critical heat flux, high heat flux, micro-channel, passive cooling, phase change, pumpless loop, pressure drop.**

NOMENCLATURE

a	Fin width.
A_c	Flow area associated with boiler gap adjacent to boiling surface.
A_s	Planform area of boiling surface, L^2.
b	Fin spacing.
Bo	Bond number defined in (1).
c	Fin height.
D	Hydraulic diameter associated with boiler gap adjacent to boiling surface, $4A_c/p$.
d	Inner diameter of tubing used in cooling loop.
d_b	Bubble departure diameter.
f	Single-phase friction factor.
f_{TP}	Two-phase friction factor.
g	Acceleration due to gravity.
H	Height of liquid in reservoir.
h_{fg}	Latent heat of vaporization.
L	Square dimension of boiling surface (21.3 mm).
L_1, L_2, L_3	Lengths of tubing sections indicated in Fig. 8.
$\dot{m}$	Mass flow rate induced in loop.
P	Pressure.
p	perimeter of flow gap.
ΔP	Pressure drop.
ΔP_*	Total liquid head of pumpless loop.
ΔP_A	Accelerational pressure drop.
ΔP_F	Frictional pressure drop.
ΔP_G	Gravitational pressure drop.
q''	Heat flux based on planform area (L^2) of heater.
q''_m	Critical heat flux based on planform area (L^2) of heater.
Re_d	Reynolds number associated with liquid flow in tubing, $4\dot{m}/(\pi d\mu_f)$.
T	Temperature.
u_L	Two-phase mixture velocity at exit from boiling surface.
v	Specific volume.
v_{fg}	Specific volume difference between vapor and liquid.
x	Thermodynamic equilibrium quality.
x_L	Thermodynamic equilibrium quality at exit from boiling surface.

Greek Symbols

α	Void fraction.
δ	Thickness of boiler gap.
θ	Contact angle.
μ	Viscosity.
ρ	Density.
σ	Surface tension.

Subscripts

0,1,2,3,4	Reference points in cooling loop defined in Fig. 8.
A	Accelerational.
f	Liquid.
F	Frictional.
fg	Difference between vapor and liquid.
g	Vapor.
G	Gravitational.
$i \rightarrow j$	Between points i and j, $i = 0-4$, $j = 0-4$.
L	Exit from boiling surface (point 4 in Fig. 8).
m	Maximum, CHF condition.

Manuscript received June 1, 2002; revised January 10, 2003. This work was supported by the Office of Basic Energy Sciences of the U.S. Department of Energy under Award DE-FG02-93ER14394-A7. This work was presented at the I-Therm 2002 International Conference on Thermal, Mechanics and Thermo-mechanical Phenomena in Electronic Systems, San Diego, CA, May 29-June 1, 2002. This work was recommended for publication by Associate Editor C. H. Amon upon evaluation of the reviewers' comments.

The authors are with the International Electronic Cooling Alliance, Purdue University, West Lafayette, IN 47907 USA (e-mail mudawar@ecn.purdue.edu).

Digital Object Identifier 10.1109/TCAPT.2003.811478

out Exit from boiling surface.
w Flat boiling surface or flush-mounted base of enhanced surface.
z Distance along direction of fluid flow.

I. Introduction

LIQUID cooling has always been viewed as the logical progression from air cooling as heat dissipation levels prevalent in electronic devices and systems continue to escalate. However, many computer manufacturers are presently reluctant to take any steps away from air cooling because of concerns over both the reliability of liquid cooling systems and high cost of transitioning to, and implementing liquid cooling technology. The trade-off between the need to dissipate the ever increasing device heat fluxes and maintaining low cost makes future cooling solutions quite elusive, especially when one considers the shrinking profit margins in the entire electronics industry.

Poor thermal transport properties of air are responsible for a large device-to-air thermal resistance, which can lead to very high device temperatures when dissipating high heat fluxes. Some improvement is possible with high-performance heat sink attachments, better interface materials and use of multiple air fans, but limits to the device temperature have already been reached and any further escalation in heat flux will result in unacceptably high device temperatures.

Liquid cooling will undoubtedly alleviate those high device temperature concerns, and cooling options with liquids are abound. However, all liquid cooling solutions share a number of serious drawbacks—sealing problems, high cost, reduced reliability, and, for many, the need for a pump, which further compounds the cost and reliability concerns. Both water and fluorochemicals have been investigated and, in a few cases, implemented in electronic cooling systems. Water has excellent thermal transport properties but, owing to its poor dielectric properties, cannot be used in direct contact with current-carrying components. Hence, water is only used in closed, indirect cooling systems, buffered from the device surface by a multi-layer consisting at a bare minimum of a metallic shell and a thermally-conducting interface material. Hence, while water can greatly enhance convective cooling effectiveness, the combined thermal resistance of the buffer layers can elevate device temperature when dissipating high heat fluxes.

Fluorichemicals such as 3M's Fluroinerts are especially popular for electronic cooling because their superior dielectric properties facilitate direct immersion of the device in the liquid coolant, completely eliminating the thermal resistance of the buffer layers required with water-cooled systems. Unfortunately, the thermal properties (especially thermal conductivity and latent heat of vaporization) of those coolants are far inferior to those of water. Thus, there is a need to greatly enhance their cooling effectiveness using such means as high coolant velocities, surface augmentation, and, especially, change of phase.

Boiling is a simple yet very effective means for enhancing Fluorinert cooling performance. It has been successfully demonstrated in a wide variety of configurations, including pool boiling thermosyphons, channel flow, jet-impingement and spray [1]. Pool boiling thermosyphons are of particular interest for the first generation of direct-immersion liquid cooling systems. It features simplicity of design, ease of fabrication (compared to flow boiling systems), maintenance-free operation, and, most importantly, natural circulation without the need for a pump. One of the important cooling limits of a pool boiling thermosyphon is critical heat flux (CHF). Without surface augmentation or subcooling, CHF in a large pool of saturated of FC-72 is less than 20 W.cm^{-2} [2], [3]. Given the stringent volume constraints of electronic cooling hardware, only a small mass of the dielectric liquid may be permitted, and the small confines of the liquid pool can have a strong bearing on the liquid replenishment of the device surface during vigorous boiling, which greatly diminishes CHF and endangers device integrity.

Those drawbacks, and the need to miniature cooling hardware, have brought micro-channel and mini-channel cooling to the forefront of direct liquid-immersion cooling techniques. Micro-channel cooling loops feature very high cooling performance, compact design, and small coolant inventory [4]–[7]. However, forcing a liquid or two-phase mixture through very small channels creates considerable pressure drop. Hence, much attention has been given in recent years to the development of a low flow rate micro-pump that is capable of handling high pressure drops. Obvious obstacles have been the high cost and, more importantly, limited reliability of those micro-pumps.

This study explores means of incorporating micro-channel and mini-channel cooling using a pumpless, self-sustaining flow loop. This loop is examined as alternative to conventional thermosyphon cooling systems. Tests were conducted to determine upper cooling limits from simulated high-heat-flux devices with flat, micro-channel and mini-channel surfaces. Similar surfaces have been examined in the past in conjunction with both pool boiling [2], [8] and channel flow boiling systems [9]. Key objectives of this study are to

1) assess the feasibility of the pumpless flow boiling loop;
2) explore upper cooling limits using flat, micro-channel and mini-channel surfaces;
3) examine analytically the coolant flow rate requirements and pressure drop trends for different boiler geometries.

II. Experimental Methods

A. Pumpless Loop Concept

The pumpless loop concept relies on fluid density differences between two vertical, parallel tubes to induce fluid motion. As shown in Fig. 1, the device surface forms a side wall to a miniature rectangular boiler which is connected to the bottom of the hot tube. The top ends of both tubes are connected to a liquid reservoir, maintaining a constant near-ambient pressure. The vapor exiting the boiler and ascending through the hot tube bubbles through the reservoir liquid and rises into an air-cooled condenser situated directly above the liquid reservoir. The vapor is condensed into liquid droplets that drip down into the reservoir. The vapor bubbles exiting the boiler greatly reduce the density of the two-phase mixture in the hot tube. Large density differences are therefore incurred between liquid in the cold tube and

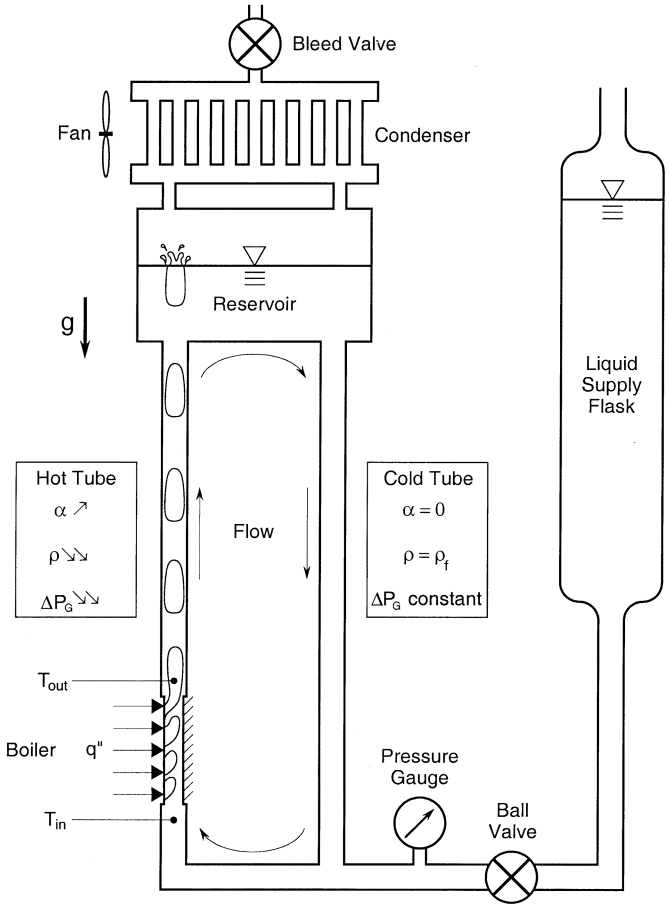

Fig. 1. Pumpless loop cooling concept and experimental setup.

two-phase mixture in the hot tube. This sets up a nonequilibrium in hydrostatic pressure at the lower junction between the two tubes, causing the denser liquid to flow downwards in the cold tube to compensate for the two-phase upflow in the hot tube. This constitutes a flow loop which is controlled entirely by density differences and, hence, heat dissipation from the device.

This pumpless loop constitutes a "smart" cooling system which enhances its own performance in response to an increase in device heat flux. This feature is inherent in the system and functions without external aid such as a pump. An increase in heat flux causes a larger vapor void fraction in the hot tube, inducing even larger density differences between the two tubes, and increasing the velocity of the two-phase mixture in the boiler. This system combines many attributes that are important to electronic cooling. It uses dielectric coolant (FC-72) for direct immersion cooling, does not require a pump, is self-driven and self-sustaining, requires a small coolant inventory, and, as demonstrated later in this paper, greatly enhances CHF relative to pool boiling thermosyphons. Eliminating the need for a pump reduces system cost considerably and enhances cooling system reliability.

There are two fundamental differences between this pumpless loop and pool boiling thermosyphons, both differences are related to the manner in which replenishment liquid is returned to the boiling surface to compensate for the vapor produced. First, liquid in a thermosyphon has to penetrate downwards between rising bubbles to reach the boiling surface, whereas the pumpless loop completely isolates the return path of the replenishment liquid from that of the vapor. A second difference is the effect of boiler size on the boiling process. The small confines of a compact boiler in a pool boiling thermosyphon can greatly influence both bubble release and liquid return, which can have a detrimental effect on CHF. The pumpless loop circumvents this problem by relying on induced channel flow boiling, which is far less sensitive to boiler size, and may actually benefit from the increased flow velocity in a narrow gap [10]–[12].

B. Boiler Design

As shown in Fig. 2(a), the boiler test module consisted of a vertical heated surface encased in a rectangular G-10 fiberglass plastic housing and facing a transparent polycarbonate cover plate. Different cover plates were fabricated to vary the boiler's gap between the boiling surface and cover plate.

Fig. 2(b) shows the construction of the heating block attached to the boiler. The heating block was constructed of a cylindrical oxygen-free copper rod with 16 cartridge heaters. The portion of the heating block facing the boiler was machined down to a square cross-section, terminating with a 21.3×21.3 mm^2 boiling surface that simulated a computer processor or other high heat flux device. Three type-K thermocouples recorded the liquid temperature at the boiler inlet, the temperature of the flat boiling surface or base temperature of the enhanced surface, and the temperature of the two-phase mixture just emerging from the boiling surface.

Fig. 3 shows the details of the enhancement features on the micro-channel and mini-channel surfaces. The flat surface was flush-mounted in a raised platform inside the G-10 housing as illustrated in Fig. 2(a). For the enhanced surfaces, the base of the micro-fins was flush with the raised platform. The boiler gap, δ, is the defined in the present study as the distance from the transparent cover to the boiling surface itself for the flat surface, and to the top of the fins for the enhances surfaces. All boiling surfaces were blasted with 1200 grit particles to ensure uniform micro-texture.

C. Experimental Procedure

The loop was filled to a predetermined reservoir level with liquid from a graduated supply flask as shown in Fig. 1. The supply flask valve was closed during every test run. A deaeration procedure consisting of vigorous boiling and condensation was adopted before each test. The test commenced by starting the condenser fan and supplying very low power to the cartridge heaters from a variable voltage transformer. The power was incremented slowly thereafter, ensuring steady-state conditions were reached between increments. The waiting period between power increments varied according to heat flux: 20 to 90 min below 50% CHF, down to about 5 min above 90% CHF. The test run was terminated once CHF was detected. Temperatures were recorded by an Hewlett Packard 3497A data acquisition system which was interfaced to a PC. The electrical power supply was measured by a Yokogawa power meter.

Repeatability in CHF measurements was confirmed to within 2.2% for all boiling surfaces by executing three tests for each boiler gap. Power readings were accurate to within 0.02% and

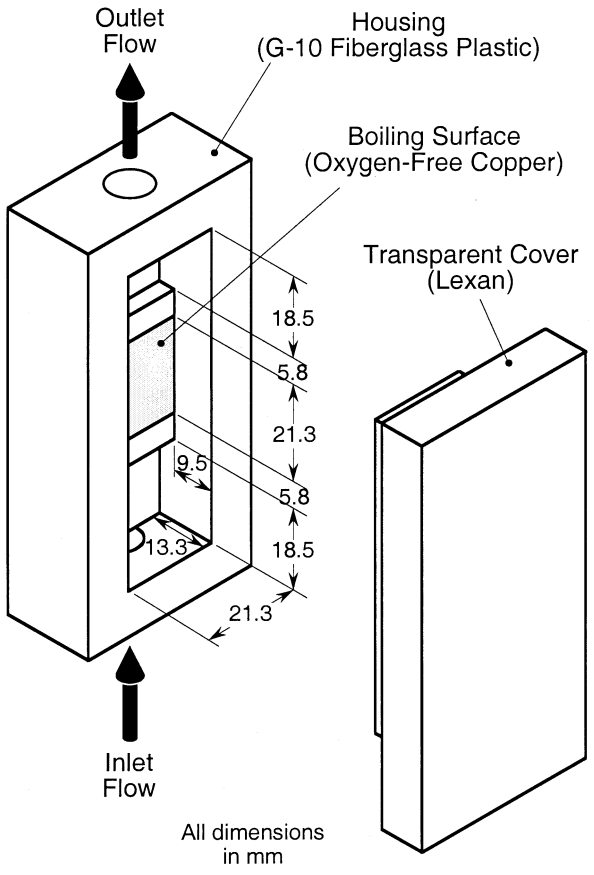

(a)

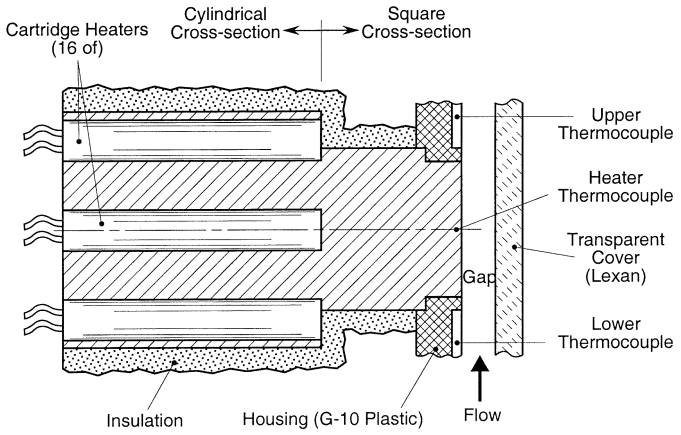

(b)

Fig. 2. (a) Housing and (b) cross-sectional view of test module. Shown is the flat surface without micro-channel or mini-channel enhancement.

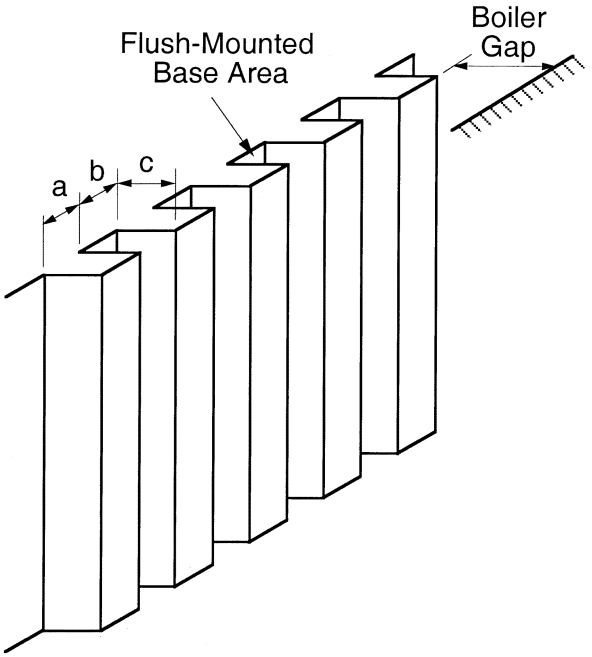

(a)

Dimension	Micro-channel Surface	Mini-channel Surface
Fin width, a	0.20 mm	1.98 mm
Fin spacing, b	0.20 mm	1.57 mm
Fin height, c	0.66 mm	3.05 mm

(b)

Fig. 3. Micro-channel and mini-channel enhancement features.

heat loss was less than 2% of the electrical power input. Accuracy of the temperature measurements was better than 1.0 °C.

III. Results and Discussion

A. FC-72 Versus Water Results for Flat Surface

As indicated earlier, far lower cooling rates are possible with FC-72 than with water because of the drastic differences in thermophysical properties. In a recent study by the authors [12], the boiler gap was varied over a wide range, from 0.13 to 21.5 mm, and CHF measured and compared for the two fluids. Fig. 4 shows CHF is unaffected by boiler gap for gaps over 0.51 mm for water and 3.56 mm for FC-72. Decreasing the gap below those values produced drastic, yet opposite trends in CHF for the two fluids. These results appear contradictory at first, but can be easily explained by the larger differences in both surface tension and contact angle between the two fluids. It is well known that CHF occurs when the replenishment liquid flow to the boiling surface in interrupted. Photographic studies in [12] showed bubbles in FC-72 were quite small, allowing liquid replenishment even in very narrow boiler gaps. Decreasing the gap accelerates the two-phase mixture along the boiling surface leading to further CHF enhancement. Water tests produced much larger vapor bubbles which were squeezed against the transparent cover and spread laterally for small gaps, blocking liquid replenishment to the boiling surface as illustrated in Fig. 4. Small gaps were therefore very advantageous for FC-72 but detrimental for water.

Fig. 5 illustrates the dramatic differences in bubble departure diameter for FC-72 and water according to the Fritz Bond number correlation [13]

$$Bo \equiv \frac{g(\rho_f - \rho_g)d_b^2}{\sigma} = 4.33 \times 10^{-4}\theta^2 \qquad (1)$$

where θ is the contact angle in degrees. Those differences are largely due to nearly an order-of-magnitude greater surface tension and larger contact angle for water compared to FC-72,

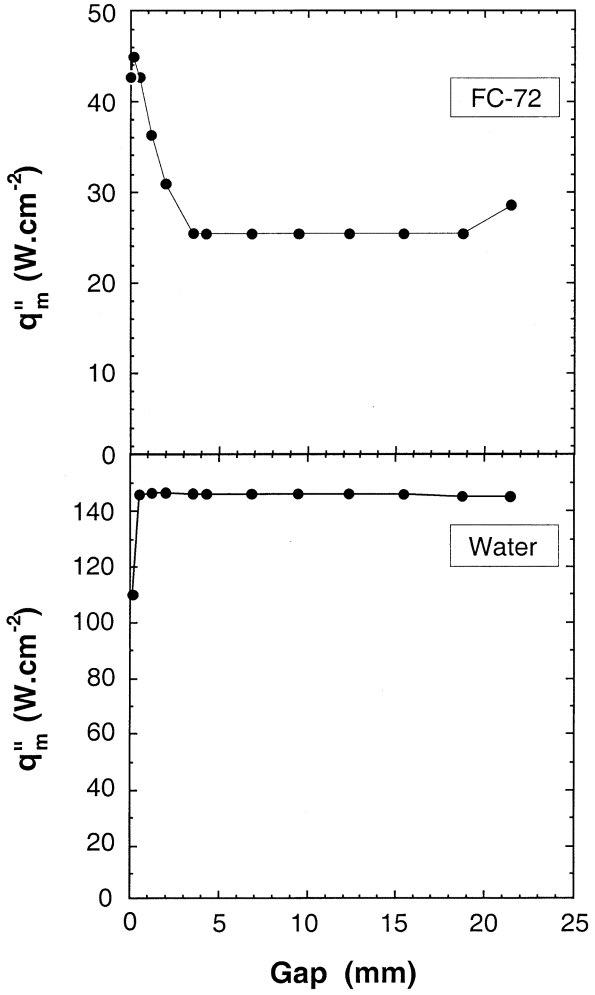

Fig. 4. Variation of flat surface CHF data with boiler gap for FC-72 and water (adapted from Mukherjee and Mudawar [12]).

whose contact angle in vanishingly small on most practical surfaces. It is important to note that (1) is used here only as an approximate measure for bubble departure diameter. More accurate estimates of bubble diameter should take into consideration the drag forces exerted by the liquid in the boiler gap. Equating the drag force to the surface tension force yields a bubble departure diameter inversely proportional to the square of liquid velocity. Decreasing boiler gap increases two-phase velocity, resulting in even smaller bubbles in FC-72 than predicted according to (1), hence allowing both the bubbles and replenishment liquid to pass unhindered even in small gaps, and resulting in higher CHF.

These findings prove that FC-72 and as well as other coolants with small surface tension and small contact angle are well suited to micro-channel flow, given the small obstruction vapor bubbles create to the liquid flow. However, with a further decrease in boiler gap, a point must be reached where even the small bubbles in such coolants begin to block the liquid flow, which is clearly manifest in Fig. 4 by a decrease in CHF below a gap of 0.13 mm.

The small contact angle of FC-72 provides another heat transfer advantage, namely a very thin liquid film along the perimeter of bubbles.

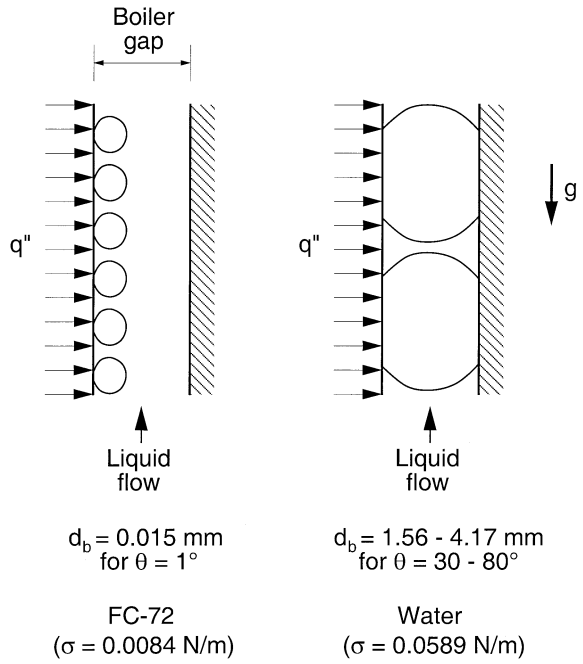

Fig. 5. Limited blockage of replenishment liquid flow in boiler gap in FC-72 compared to significant blockage in water due the large differences in bubble departure size (predicted according to Fritz correlation [13]) between the two fluids.

B. FC-72 Results for Flat and Enhanced Surfaces

Since smaller gaps produced the highest CHF values for FC-72 in [12], it was decided in the present study to investigate only small gaps when exploring CHF from enhanced surfaces. Fig. 6(a) and 6(b) show boiling curves for the flat, micro-channel and mini-channel surfaces corresponding to boiler gaps of 0.13–0.25 and 1.27–1.52 mm, respectively.

All boiling curves show a smooth transition between the single-phase liquid region and nucleate boiling region. Absent is the large temperature drop commonly observed in pool boiling, which can be very damaging to temperature sensitive devices [2]. For the smaller gap range, the micro-channel surface showed the greatest enhancement in nucleate boiling, evidenced by a leftward shift to lower surface superheat values, followed by the mini-channel and flat surfaces. For the higher gap range, the flat and micro-channel surfaces produced competing nucleate boiling results, while the mini-channel surface resulted in the highest superheat. It is evident the added flow resistance with the larger mini-channel fins causes preferential liquid flow in the larger gaps away from the fins.

Fig. 7 compares CHF results for the flat, micro-channel and mini-channel surfaces within a small gap range of 0.13 to 1.52 mm. Clearly, the two enhanced surfaces provide CHF values that are superior to those of the flat. The mini-channel surface follows the same CHF trend with boiler gap as the flat surface, but with a 38% enhancement. This implies the mini-channel, with its relatively wide surface flow features is equivalent to a flat surface with greater heat transfer area, but sharing the same base area. Both the flat and mini-channel surfaces seem to benefit from an increasing two-phase mixture velocity with decreasing boiler gap. Both surfaces also possess a crossover boiler gap (corresponding to maximum CHF) of

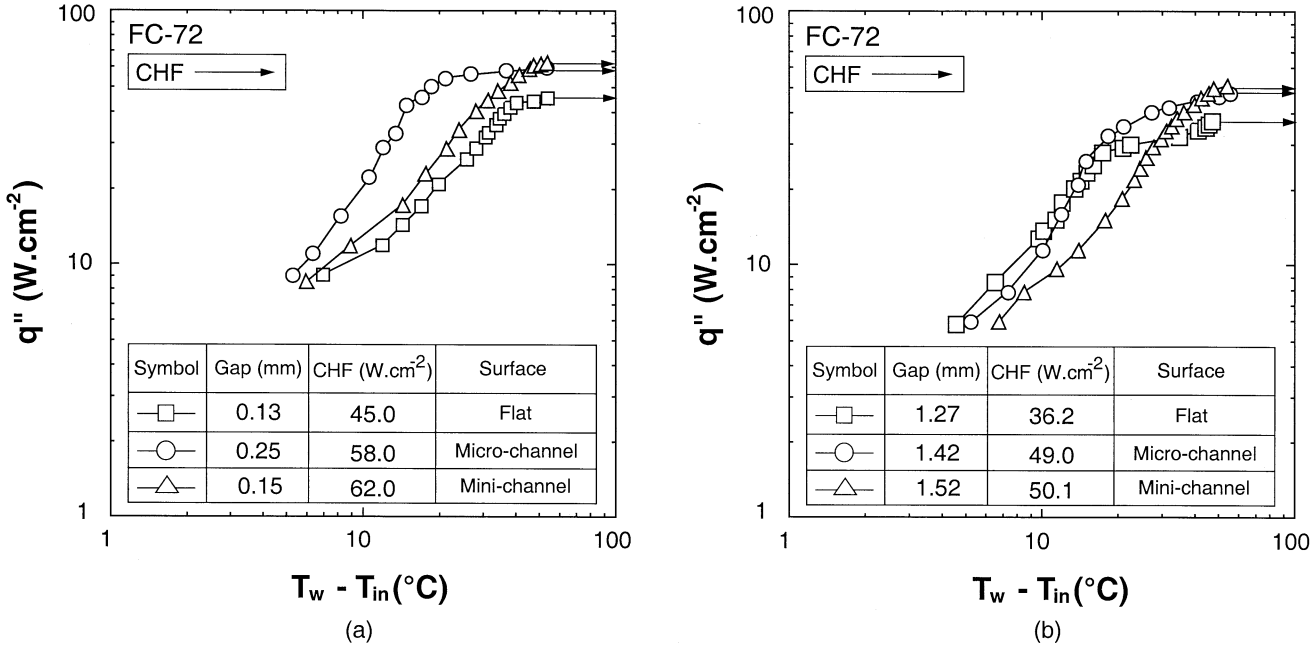

Fig. 6. Boiling curves for flat, micro-channel and mini-channel surfaces for boiler gap ranges of (a) 0.13–0.25 mm and (b) 1.27–1.52 mm.

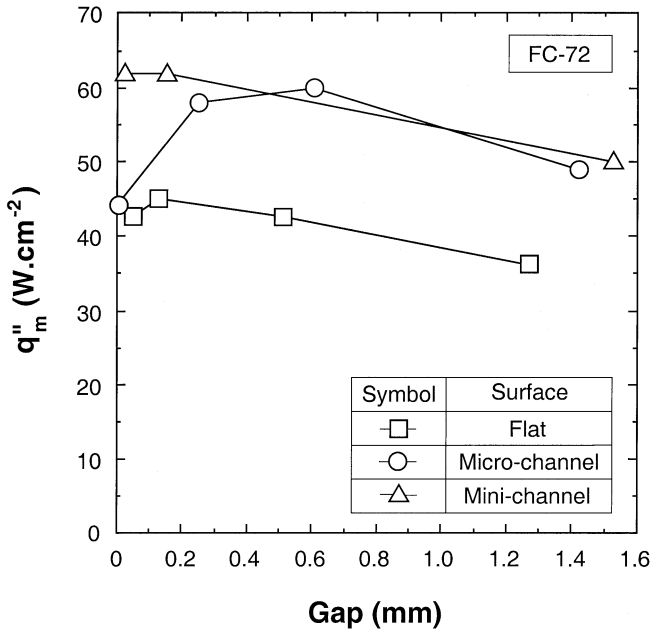

Fig. 7. Variation of CHF data with boiler gap for FC-72 on flat, micro-channel, and mini-channel surfaces.

about 0.14 mm below which CHF no longer increases with decreasing gap. The fact that the crossover points for both the flat and mini-channel surfaces are nearly the same lends credence to the similarities in CHF mechanisms between the two surfaces. One key difference, however, is that CHF is compromised to lower values below the crossover point for the flat surface, Fig. 7, while it stays about the same for the mini-channel. This may be the result of the crossover gap beginning to interfere with bubble growth and interrupt replenishment liquid flow over the flat surface. The same conditions were observed over the top surfaces of the mini-channel fins, but the open areas between the fins provided ample flow space for the liquid.

Fig. 7 shows the crossover gap effect is both far stronger and occurs at a larger gap with the micro-channel surface than with the other two. The obvious difference in CHF trends between the micro-channel and mini-channel surfaces is related to the inability of the small areas between micro-channel fins to provide adequate spaces for the replenishment liquid flow. A key practical advantage with the micro-channel surface, however, is the ability to form the surface features directly into the device surface, whereas the larger mini-channel features have to be formed into a separate plate that is attached onto the device surface, introducing an added thermal contact resistance.

Overall, decreasing boiler gap seems to precipitate an increase in CHF due to increased two-phase flow velocity along the boiling surface. The small surface tension and contact angle of FC-72 enable bubbles to pass through very small gaps. The increase in flow velocity with decreasing gap also helps decrease bubble size further. This continues until a crossover gap size is reached below which the bubbles will begin to obstruct the flow.

C. Pumpless Loop Versus Pool Boiling CHF

As indicated earlier in this paper, the present pumpless loop is a prime contender to the pool boiling thermosyphon. A key drawback of the thermosyphon's boiler is CHF sensitivity to boiler dimensions, since replenishment liquid has to penetrate downwards between rising bubbles in the same boiler cavity, and a narrow cavity in a miniature boiler could greatly obstruct the liquid replenishment. The pumpless loop, on the other hand, separates the path of replenishment liquid from the rising bubbles, minimizing obstruction to the liquid flow. Thus, the pumpless loop is far more tolerant of narrow gap boilers than a pool boiling thermosyphon is.

To prove this point, the present pumpless loop apparatus was modified by disconnecting the cold tube shown in Fig. 1 entirely, thereby reducing the system to a simple pool boiling ther-

TABLE I
COMPARISON OF CHF FROM FLAT SURFACE IN FC-72 IN PUMPLESS LOOP AND POOL BOILING FOR DIFFERENT GAPS

Gap (mm)	Measured pool boiling CHF[a] ($W.cm^{-2}$)	Measured pumpless loop CHF ($W.cm^{-2}$)	Ratio of pumpless loop to pool boiling CHF
0.13	10.1	45.0	4.46
0.51	12.1	42.6	3.52
1.27	13.6	36.2	2.66
3.56	13.6	25.5	1.88
12.32	13.8	25.5	1.85

a Pool boiling CHF for FC-72 according to the Zuber et al. [14] correlation is 15.24 $W.cm^{-2}$

mosyphon. Table I compares the measured pool boiling CHF data for a flat surface in FC-72 to the pumpless loop flat surface data, and the CHF prediction for FC-72 based on the Zuber *et al.* model [14] for an infinite liquid pool

$$q''_m = 0.131\rho_g h_{fg}\left[\frac{\sigma(\rho_f-\rho_g)g}{\rho_g^2}\right]^{1/4}. \tag{2}$$

Notice first the pool boiling data are all smaller than the model predicts, and decrease with decreasing gap. On the other hand, the pumpless loop CHF data show a monotonic increase as the gap is decreased from 12.32 to 0.13 mm. More importantly, the ratio of pumpless loop to pool boiling CHF increases from 1.85 for $\delta = 12.32$ mm to 4.46 for $\delta = 0.13$ mm. As shown in Fig. 7, the flat, mini-channel and micro-channel surfaces yield maximum CHF values of 45.0, 62.0, and 60.0 $W.cm^{-2}$, respectively, which are 4.5, 5.9, and 5.7 times greater than for pool boiling from a flat surface for corresponding gaps.

There results reveal

a) CHF with the present pumpless loop is superior to that with pool boiling;
b) considerable additional CHF enhancement is possible with the small gaps desired for miniature electronic cooling systems;
c) very small coolant inventory is needed to accomplish this goal.

It is important to note that these attractive CHF results by no means constitute an upper limit for electronic cooling using the pumpless loop. Far greater device heat fluxes are possible by attaching the device to a metallic plate (flat or enhanced) which would form the boiling surface in the pumpless loop's boiler. Thus, the maximum device heat flux can be several multiples of the CHF values measured in this study.

IV. PRESSURE DROP MODEL OF PUMPLESS LOOP

A. Model Formulation

It is imperative that in order to understand how the pumpless loop functions for different boiler gaps with increasing heat flux, all the forces influencing the loop performance must be carefully examined. A pressure drop model was developed for this purpose, which facilitates the assessment of boiler gap variations on various components of pressure drop, coolant mass flow rate, and boiling surface inlet and exit velocities. Those same trends are used to explain the effect of boiler gap on CHF.

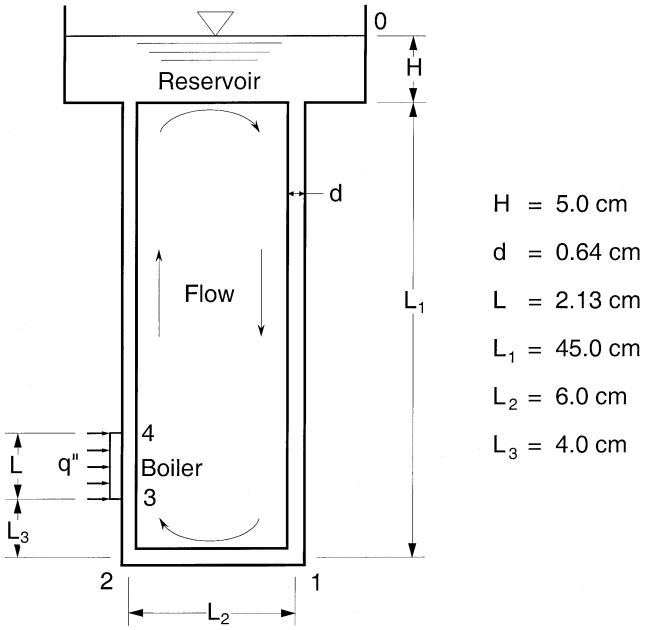

Fig. 8. Nomenclature used in pressure drop model, and dimensions of geometrical parameters of pumpless loop.

Fig. 8 shows the nomenclature used in this model as well as key pumpless loop dimensions. Pressure drop in this system includes frictional, accelerational, and gravitational components. Accelerational pressure drop is encountered only along the boiling surface, where phase change and, hence, flow acceleration, take effect. Salient assumptions used in this model are negligible pressure losses due to the tube bends as well as to the boiler and reservoir inlet and exit effects.

A constant datum pressure P_0 is assumed at the free interface of liquid in the reservoir, and pressure drops in the individual portions of the loop are represented as

$$P_0 - P_1 = \Delta P_{F,0\to1} - \rho_f g(H + L_1) \tag{3}$$

$$P_1 - P_2 = \Delta P_{F,1\to2} \tag{4}$$

$$P_2 - P_3 = \Delta P_{F,2\to3} + \rho_f g L_3 \tag{5}$$

$$P_3 - P_4 = \Delta P_{F,3\to4} + \Delta P_{A,3\to4} + \Delta P_{G,3\to4} \tag{6}$$

$$P_4 - P_0 = \Delta P_{F,4\to0} + \Delta P_{G,4\to0}. \tag{7}$$

Adding (3) to (7), and rearranging

$$\begin{aligned}\Delta P_* &= \rho_f g(H + L_1 - L_3)\\ &= (\Delta P_{F,0\to1} + \Delta P_{F,1\to2} + \Delta P_{F,2\to3}) + \Delta P_{F,3\to4}\\ &\quad + \Delta P_{F,4\to0} + \Delta P_{A,3\to4} + \Delta P_{G,3\to4} + \Delta P_{G,4\to0}.\end{aligned} \tag{8}$$

The left-hand side term ΔP_* of (8) is the total pressure drop due to the liquid head only, which balances the remaining gravitational, accelerational and frictional pressure drops across the entire loop.

The frictional pressure drops resulting from single-phase flow at flow rate $\dot{m}$ inside the plastic tubing of diameter d can be combined into one term

$$\Delta P_{F,0\to1}+\Delta P_{F,1\to2}+\Delta P_{F,2\to3} = f\left[\frac{\rho_f}{2}\right]\left[\frac{\dot{m}}{\rho_f\frac{\pi d^2}{4}}\right]^2\left[\frac{L_1+L_2+L_3}{d}\right] \quad (9a)$$

where [15]

$$f=\frac{64}{Re_d} \qquad \text{for } Re_d<2000 \quad (9b)$$

$$f=0.316\,Re_d^{-1/4} \qquad \text{for } 2000<Re_d<2\times10^4 \quad (9c)$$

$$f=[0.79\ln Re_d-1.64]^{-2} \qquad \text{for } 2\times10^4<Re_d<5\times10^6. \quad (9d)$$

The Petukhov correlation [16], (9d), is actually valid for Reynolds number values from 3000 to 5×10^6. However, it is used here only for $Re_d>2\times10^4$ since (9c) is more appropriate for the lower range of the turbulent region.

The homogeneous equilibrium model [5]–[7], [17] is used to determine the two-phase frictional, accelerational, and gravitational components of pressure drop. A key attribute of the homogeneous equilibrium model is its ability to provide analytical expressions for two-phase pressure drop.

The two-phase regions in the cooling loop have a clear demarcation—the first region is the heated region (3 to 4) corresponding to the boiling surface itself, and the second an adiabatic two-phase region (4 to 0). At the outlet from the boiling surface (4), the thermodynamic equilibrium quality is expressed as

$$x_L=\frac{q''A_s}{\dot{m}h_{fg}} \quad (10)$$

where A_s is the planform area (L^2) of the boiling surface. Since thermodynamic equilibrium quality x has a linear relationship with distance z along the boiling surface, the two-phase frictional pressure drop across the boiling surface can be expressed as

$$\Delta P_{F,3\to4}=2f_{TP}v_f\left(\frac{\dot{m}}{A_c}\right)^2\left[1+\frac{x_L}{2}\frac{v_{fg}}{v_f}\right]\frac{L}{D} \quad (11)$$

where A_c is the flow area associated with the flow gap, D is the hydraulic diameter of the boiler gap, and f_{TP} is the two-phase friction factor, which is set equal to 0.003 [17].

Since x is constant $(=x_L)$ along the adiabatic two-phase region, the two-phase frictional pressure drop between points 4 and 0 can be expressed as

$$\Delta P_{F,4\to0}=2f_{TP}v_f\left(\frac{\dot{m}}{\rho_f\frac{\pi d^2}{4}}\right)^2\left[1+x_L\frac{v_{fg}}{v_f}\right]\left[\frac{L_1-L_3-L}{d}\right]. \quad (12)$$

The homogeneous equilibrium model yields the following expressions for the two-phase gravitational pressure drop across the boiling surface (3–4), where x varies linearly with z, and the adiabatic section (4–0), where $x=x_L$, respectively

$$\Delta P_{G,3\to4}=\int_3^4\left\{\frac{g}{v_f+xv_{fg}}\right\}dz=\frac{gL}{v_{fg}x_L}\ln\left\{1+x_L\frac{v_{fg}}{v_f}\right\}, \quad (13)$$

$$\Delta P_{G,4\to0}=\int_4^0\left\{\frac{g}{v_f+xv_{fg}}\right\}dz=\frac{g(H+L_1-L_3-L)}{v_f+x_Lv_{fg}}. \quad (14)$$

Since x varies linearly with z along the boiling surface, the accelerational pressure drop across the heated surface can be expressed as [5]–[7]

$$\Delta P_{A,3\to4}=\left\{\left(\frac{\dot{m}}{A_c}\right)^2(v_f+xv_{fg})\right\}\Bigg|_3^4=v_{fg}\left(\frac{\dot{m}}{A_c}\right)^2x_L. \quad (15)$$

Equation (8) was used to ascertain the effects of boiler gap on the various components of pressure drop. The variables examined also include the mass flow rate induced in the loop, $\dot{m}$, the liquid velocity at the inlet to the boiling surface, $u_{in}(=\dot{m}/(\rho_f A_c))$, and the velocity of the two-phase mixture exiting the boiling surface, u_L, which is given by

$$u_L=\left(\frac{\dot{m}}{A_c}\right)(v_f+x_Lv_{fg}). \quad (16)$$

The cooling loop performance was evaluated at CHF as well as for successive heat flux levels, under saturated conditions corresponding to one atmosphere.

The reader should refer to the previous study by the authors [12] for a more comprehensive pressure drop assessment for the flat surface using the Drift-flux model which, unlike the homogeneous equilibrium model, accounts for the complex velocity differences between the phases.

B. Model Results

Fig. 9(a)–(c) show the model predictions for FC-72 corresponding to the measured CHF for each gap for the flat, micro-channel and mini-channel surfaces, respectively. Trends of important loop variables with boiler gap are manifest in the CHF trends, which are provided in the top plot of each figure. Some of the trends are shared by all three surfaces. For all three surfaces, the frictional pressure drop from 0 to 3 is quite small over the range of gaps tested. A few salient differences in the physical trends among the three surfaces are evident from the model predictions. For the mini-channel surface, except for the accelerational pressure drop (3–4) and the two-phase frictional pressure drop from 4 to 0, all remaining pressure drops can, for all purposes, be considered negligible. The two dominant pressure drops more or less balance each other; as the gap increases, the two-phase frictional pressure drop increases at the expense of the accelerational. However, for the flat and micro-channel surfaces, there appear to be three regions of interest. For gaps smaller than 0.2 mm, the accelerational and frictional pressure drops associated with the boiling surface itself (3–4) add up to nearly the entire available liquid head, with the former gaining at the expense of the latter as the gap increases. All other pressure

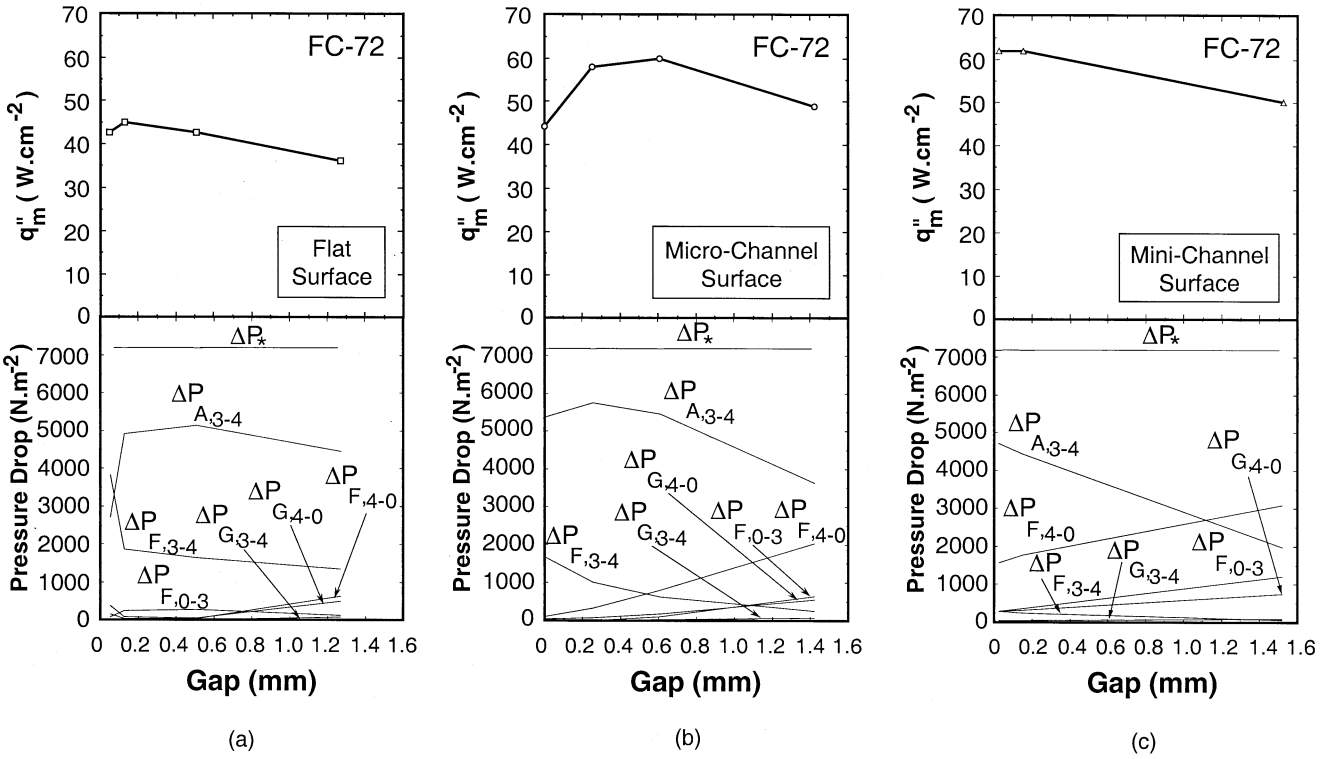

Fig. 9. Pressure drop model predictions for: (a) flat, (b) micro-channel, and (c) mini-channel surfaces. The top plot in each figure includes the measured CHF data for reference.

drops in this range appear inconsequential. The second range is from 0.2 to 0.5 mm, where the same trends are observed as in the previous range but the rate of change of the two dominant pressure drop terms is relatively mild. In the third range from 0.5 to 1.5 mm, the two dominant pressure drops show a constant rate of descent with increasing gap, with the two-phase frictional pressure drop across the adiabatic length (4–0) taking up the descent. An interesting point to note is that the enhanced surfaces appear to be subjected to greater two-phase friction across the adiabatic length (4–0) than the flat surface, especially with larger gaps.

Of paramount importance to the results shown in Fig. 9(a)–(c) is the similarity of CHF variations with boiler gap and the variations of accelerational pressure drop associated with the boiling surface (3–4). Clearly, acceleration of the two-phase mixture with decreasing gap is key to the overall enhancement in CHF with decreasing gap. Also, limitations on two-phase mixture acceleration in very small gaps seem to correlate well with the decline in CHF for the same gaps. Furthermore, the performance of the entire system seems highly sensitive to the quantity $H + L_1 - (L + L_3)$, which accounts for the static liquid head above the boiler. While increasing this parameter can greatly enhance CHF, one must keep in mind that this parameter is dictated mostly by packaging constraints.

Earlier in this paper, the pumpless loop was described as a smart system, capable of compensating for increased heat flux (input parameter) by adjusting itself to enhance its cooling performance even further. Fig. 10(a)–(c) depict, for the flat, micro-channel, and mini-channel surfaces, respectively, the variations of mass flow rate and boiling surface exit velocity with heat flux for two select gaps per surface. The plot corresponding to each gap is terminated with the measured CHF. The mass flow rate for all three surfaces is greater for the larger gap due to larger flow area. The opposite is true for exit velocity. Fig. 10(a) shows exit velocity for the flat surface becomes constant above a heat flux of 25 W.cm^{-2} since above this flux the void fraction and thermodynamic quality both attain a value of unity, thereby yielding identical values of exit velocity. Incidentally, the difference in exit velocity between the two gaps for the flat surface is far more prominent than for the enhanced surfaces.

Figs. 9(a)–(c) and 10(a)–(c) clearly illustrate two salient advantages of a smaller gap:

a) small coolant inventory requirements;
b) augmented CHF due to high acceleration of the two-phase mixture along the boiling surface.

V. Conclusion

This study was conducted to assess the feasibility of a pumpless cooling loop for dissipating heat from a high heat flux electronic device. Experiments were performed in FC-72 using vertical flat, micro-channel and mini-channel surfaces. A pressure drop model of the entire loop was constructed using the assumptions of the homogeneous equilibrium model. The model results were used to both determine the effects of boiler gap and heat flux on key loop variables, and to help explain the measured trends of CHF with boiler gap. Key findings from the study are as follows.

1) This new cooling system is self-driven, self-sustaining, and inherently smart. It compensates for any increase in heat flux with a corresponding increase in boiling surface exit velocity, thereby enhancing performance further without external input.
2) FC-72 and other coolants with small surface tension and small contact angle (including refrigerants) are

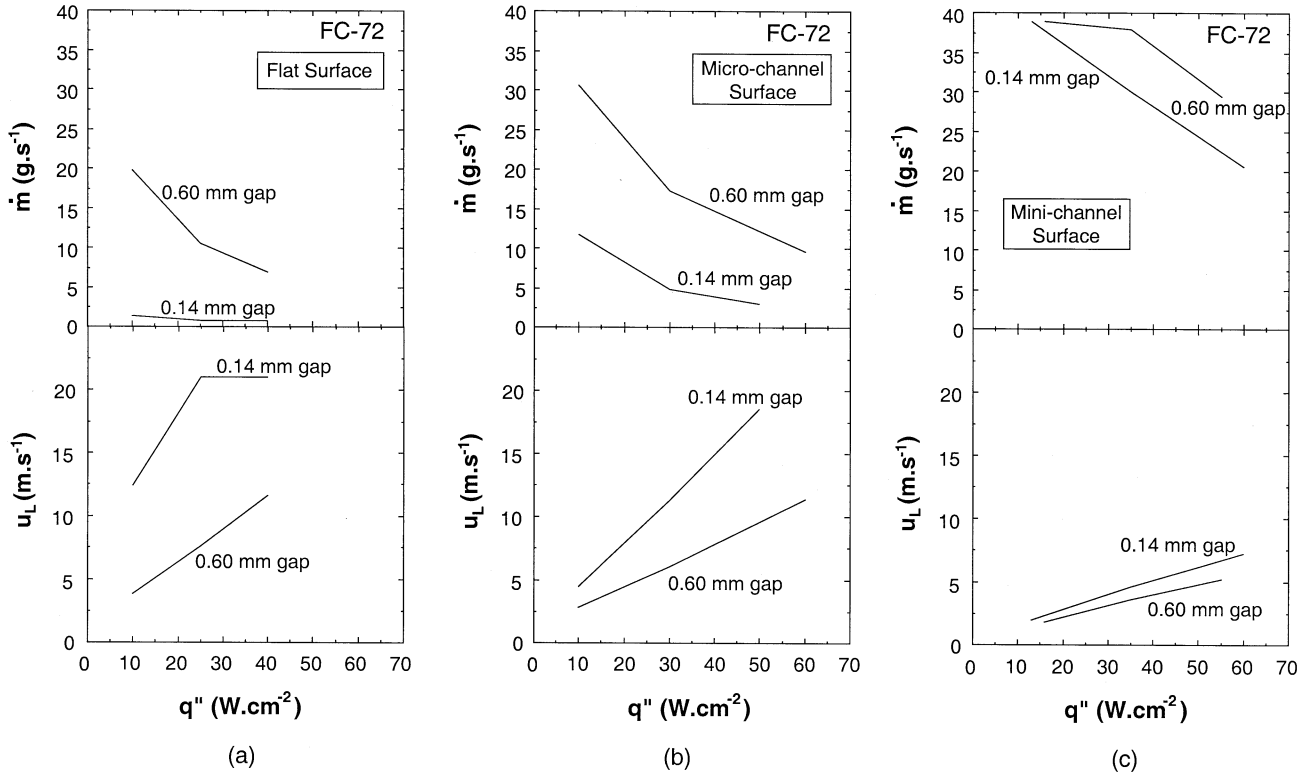

Fig. 10. Variations of predicted coolant mass flow rate and boiling surface exit velocity with heat flux and boiler gap for: (a) flat, (b) micro-channel, and (c) mini-channel surfaces.

well suited for boiling in narrow gaps. Unlike water, which forms large vapor bubbles that block the flow of replenishment liquid in the boiler, bubbles in these coolants are far smaller, offering minimal blockage even in very small gaps.

3) CHF for FC-72 generally increases with decreasing boiler gap due to increased acceleration of the two-phase mixture along the boiling surface. However, a very small crossover gap exits below which the CHF enhancement ceases to occur, as blockage begins to take effect even in FC-72.
4) The effectiveness of the pumpless loop with small gaps implies a very small coolant inventory is required to sustain this system.
5) Better nucleate boiling results are achieved with the micro-channel and mini-channel surfaces than with the flat for gaps in the range of 0.13 to 0.15 mm, but those advantages not realized with larger gaps. Absent for all surfaces is the incipient boiling temperature drop, which can be detrimental to temperature sensitive devices in pool boiling.
6) The pumpless loop is considerably superior to a pool boiling thermosyphon utilizing the same boiler geometry and same coolant. CHF values with the flat, micro-channel and mini-channel surfaces are 4.5, 5.7, and 5.9 times greater than for pool boiling from a flat surface for corresponding gaps.
7) Those CHF values constitute only baseline values for the loop performance since much greater device heat fluxes may be dissipated by attaching the device to a metallic plate possessing a much greater boiling surface area.
8) The pressure drop model shows, for small gaps, that the entire liquid head available for loop operation is used up in balancing the accelerational pressure drop, and to a lesser extent the frictional pressure drop, across the boiling surface.

REFERENCES

[1] I. Mudawar, "Assessment of high-heat-flux thermal management schemes," *IEEE Trans. Comp. Packag. Technol.*, vol. 24, pp. 122–141, 2001.
[2] T. M. Anderson and I. Mudawar, "Microelectronic cooling by enhanced pool boiling of a dielectric fluorocarbon liquid," *ASME J. Heat Transfer*, vol. 111, pp. 752–759, 1989.
[3] I. Mudawar and T. M. Anderson, "Optimization of extended surfaces for high flux chip cooling by pool boiling," *ASME J. Electron. Packag.*, vol. 115, pp. 89–100, 1993.
[4] D. B. Tuckerman and R. F. W. Pease, "High-performance heat sinking for VLSI," *IEEE Electron. Device Lett.*, vol. 2, pp. 126–129, 1981.
[5] M. B. Bowers and I. Mudawar, "Two-phase electronic cooling using mini-channel and micro-channel heat sinks—Part I. Design criteria and heat diffusion constraints," *ASME J. Electron. Packag.*, vol. 116, pp. 290–297, 1994.
[6] ——, "Two-phase electronic cooling using mini-channel and cicro-channel heat sinks—Part II. Flow rate and pressure drop constraints," *ASME J. Electron. Packag.*, vol. 116, pp. 298–305, 1994.
[7] ——, "High flux boiling in low flow rate, low pressure drop mini-channel and micro-channel heat sinks," *Int. J. Heat Mass Transfer*, vol. 37, pp. 321–332, 1994.
[8] W. Nakayama, T. Nakajimi, and S. Hirasawa, "Heat sink studs having enhanced boiling surfaces for cooling of microelectronic components," in *Proc. ASME Paper 84-WA/HT-89*, 1984.
[9] D. E. Maddox and I. Mudawar, "Single and two-phase convective heat transfer from smooth and enhanced microelectronic heat sources in a rectangular channel," *ASME J. Heat Transfer*, vol. 111, pp. 1045–1052, 1989.
[10] E. Ishibashi and K. Nishikawa, "Saturated boiling heat transfer in narrow spaces," *Int. J. Heat Mass Transfer*, vol. 12, pp. 863–894, 1969.

[11] M. Monde, "Characteristic of heat transfer enhancement due to bubbles passing through a narrow vertical channel," *ASME J. Heat Transfer*, vol. 110, pp. 1016–1019, 1988.
[12] S. Mukherjee and I. Mudawar, "Pumpless loop for narrow channel and micro-channel boiling from vertical surfaces," ASME J. Electron. Packag., to be published.
[13] W. Fritz, "Berechnung des Maximalvolume von Dampfblasen," *Phys. Z.*, vol. 36, pp. 379–388, 1935.
[14] N. Zuber, M. Tribus, and J. W. Westwater, "The hydrodynamic crisis in pool boiling of saturated and subcooled liquids," in *Proc. Int. Heat Transfer Conf.*, Boulder, CO, 1961, pp. 230–236.
[15] F. P. Incropera and D. P. Dewitt, *Fundamentals of Heat and Mass Transfer*, 4th ed. New York: Wiley, 1996, p. 460.
[16] B. S. Petukhov, "Heat transfer and friction in turbulent pipe flow with variable physical properties," in *Advances in Heat Transfer*, T. F. Irvine and J. P. Hartnett, Eds. New York: Academic, 1970, vol. 6, pp. 503–564.
[17] J. G. Collier and J. R. Thome, *Convective Boiling and Condensation*, 3rd ed. Oxford, UK: Clarendon, 1994, p. 46.

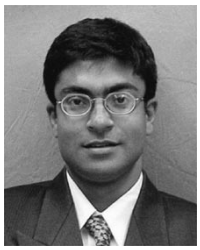

Swaraj Mukherjee received the B.S. degree in mechanical engineering from the University of Bombay, in 1998 and the M.S. degree in mechanical engineering from Purdue University, West Lafayette, IN, in 2002.

His primary research concerns electronic cooling using phase change techniques. He also has extensive fundamental and practical experience in the design of fluid and thermal systems, including refrigeration and air conditioning, centrifugal and gear pumps, and internal combustion engines.

Issam Mudawar received the M.S. and Ph.D. degrees from the Massachusetts Institute of Technology, Cambridge, in 1980 and 1984, respectively. His graduate work involved magnetohydrodynamic (MHD) energy conversion and phase-change water cooling of turbine blades.

He joined the Purdue University School of Mechanical Engineering in 1984, where he established and became Director of the Boiling and Two-Phase Flow Laboratory (BTPFL) and Electronic Cooling Research Center (ECRC). He also served as Chairman of the Heat Transfer Area, Purdue University. His work has been focused on phase change processes, thermal management of electronic and aerospace devices, intelligent materials processing, and nuclear reactor safety. His theoretical and experimental research encompasses sensible and evaporative heating of thin films, pool boiling, flow boiling, jet-impingement cooling, spray cooling, micro-channel heat sinks, heat transfer enhancement, heat transfer in rotating systems, critical heat flux, capillary pumped flows, and surface rewetting. His Electronic Cooling Research Center was renamed in 1998 as the Purdue University International Electronic Cooling Alliance (PUIECA), where efforts are presently focused entirely on high-heat-flux cooling schemes. He is also President of Mudawar Thermal Systems, Inc. (a firm that is dedicated to the development of thermal solutions to computer and aerospace systems).

Dr. Mudawar received the Best Paper Award in Electronic Cooling at the 1988 National Heat Transfer Conference, the Best Paper Award in Thermal Management at the 1992 ASME/JSME Joint Conference on Electronic Packaging, the *Journal of Electronic Packaging* Outstanding Paper of the Year Award for 1995, the Solberg Award for Best Teacher in School of Mechanical Engineering (1987, 1992, and 1996), the Charles Murphy Award for Best Teacher at Purdue University (1997), and the National Society of Black Engineers Professor of the Year Award (1985, 1987). He is a Fellow of the ASME.